



# Modelling and climatic interpretation of the length fluctuations of Glaciar Frías (north Patagonian Andes, Argentina) 1639–2009 AD

P. W. Leclercq<sup>1</sup>, P. Pitte<sup>2</sup>, R. H. Giesen<sup>1</sup>, M. H. Masiokas<sup>2</sup>, and J. Oerlemans<sup>1</sup>

<sup>1</sup>IMAU, Utrecht University, Princetonplein 5, 3584 CC Utrecht, The Netherlands

<sup>2</sup>IANIGLA, CCT Mendoza, Av Ruiz Leal s/n, 5500 Mendoza, Argentina

Correspondence to: P. W. Leclercq (p.w.leclercq@uu.nl)

Received: 16 September 2011 – Published in Clim. Past Discuss.: 26 October 2011

Revised: 9 August 2012 – Accepted: 13 August 2012 – Published: 3 September 2012

**Abstract.** We explore the climatic information contained in the record of length fluctuations of Glaciar Frías, in the north Patagonian Andes of Argentina. This record is one of the longest and most detailed glacier records in southern South America, starting in 1639. In order to interpret the length variations of Glaciar Frías since the maximum Little Ice Age extent, we use a combination of a simplified surface energy-balance model to calculate the glacier mass balance, and a flowline model to account for the dynamical response of the glacier to changes in the climatic forcing. The overall retreat of the glacier observed over 1639–2009 is best explained by an annual mean temperature increase of 1.2 °C or a decrease in annual precipitation of 34 %, most of which would have occurred during the 20th century. The glacier model is also forced with two independent tree-ring and multi-proxy reconstructions of precipitation and temperature. The uncertainties in these reconstructions are rather large, leading to a wide range in the modelled glacier length that includes most of the observations. However, in both reconstructions, the mid-17th century seems to be too cold and the early 19th century too warm to explain the observed glacier lengths with the glacier model forced with the reconstructions. Forcing with reconstructed precipitation and temperature separately shows that the influence of historical variations in precipitation on the glacier fluctuations of Glaciar Frías is smaller than that of the temperature fluctuations. This suggests that the observed 1639–2009 retreat could be best explained by a warming close to 1.2 °C.

## 1 Introduction

To understand current climate variability and to make reliable predictions of future climate change, knowledge of the past climate is needed. As instrumental measurement series have limited length, this requires the use of proxy-based information. In southern South America, long instrumental records of good quality are scarce and mostly limited to lowland, populated areas in Chile and Argentina (Rosenblüth et al., 1997). However, there is a great potential for proxy-based reconstructions of climate fluctuations in this region. Most of the available proxies in southern South America are based on dendrochronological records from the north and south Patagonian Andes, where the climate-dependent rate of growth is measured from annual tree-ring properties (e.g. ring width and density; see Boninsegna et al., 2009 for an overview). Exploiting as many independent sources as possible increases the reliability of the resulting climate reconstructions. Recently, Neukom et al. (2010, 2011) have developed a gridded dataset of precipitation and temperature anomalies in southern South America. In addition to reconstructions based on Andean tree rings, they include a variety of other proxies, such as documentary evidence, ice cores, and corals. However, the climatic information that can be derived from observed glacier length fluctuations in South America has not yet been addressed in a quantitative way. So far, this information has only been used qualitatively (e.g. Harrison et al., 2007; Neukom et al., 2011).

Usually, the high-resolution, proxy-based climate reconstructions depend on transfer functions derived from correlations with observational data. One of the benefits of this approach is that the records allow for a proper statistical

calibration and verification of the models used to develop the climate reconstructions. However, this type of reconstructions has various limitations inherent to the series available. For example, for tree-ring chronologies the capacity of capturing long-term (i.e. centennial scale) climate variability is limited by the length of the original tree-ring series and by the process of standardization intended to remove the biological trends in the records (Cook and Kairiukstis, 1990). Uncertainty in the validity of the transfer function over the entire period of reconstruction and the decrease of low frequency variability lead to increasing uncertainties in the long-term trends of reconstructed temperature and precipitation records (e.g. Briffa et al., 1998, 2001; Esper et al., 2002).

Information of glacier fluctuations can provide valuable complementary climatic information over the past centuries. Fluctuations in climate cause changes in the accumulation (snowfall) and ablation (melt) of a glacier, and thus affect the glacier mass budget. In turn, fluctuations in a glacier's mass budget lead to dynamical adjustment of the glacier geometry. The interaction between glaciers and climate is well understood, and can be described using physical relations (e.g. Oerlemans, 2001; Cook et al., 2003; Hock and Holmgren, 2005; Rye et al., 2010; Giesen and Oerlemans, 2010). Therefore, we are not dependent on empirical transfer functions when we use glacier fluctuations as a climate proxy. Despite the lower temporal resolution inherent to the response time of glaciers to climate change, past glacier fluctuations form a valuable climate proxy to complement existing temperature and precipitation reconstructions.

On centennial timescales, length fluctuations are generally the only known glacier variable. Combinations of documentary and geomorphological information have led to high-resolution glacier length records for the European Alps and Scandinavia (e.g. Zumbühl and Holzhauser, 1988; Nussbaumer et al., 2011). However, the historical evidence available for the Andes is far less extensive than for Europe. In this context, the length record of Glaciar Frías, in the Monte Tronador area in northern Patagonia, is a fairly detailed, long glacier length record (Villalba et al., 1990; Masiokas et al., 2009). In this study, we exploit this glacier length record by extracting information about the north Patagonian climate over the past four centuries.

Glacier length changes have been used previously to reconstruct climatic variations. Oerlemans (2005) and Leclercq and Oerlemans (2012) have analysed a large sample of glacier length records with a simple glacier model to reconstruct large-scale temperature fluctuations. In these studies, the influence of variations in precipitation was neglected, which is plausible for a large-scale average. For individual glaciers, local variations in precipitation cannot be neglected and this approach cannot be used. Furthermore, the simple model will likely perform poorly for an individual glacier, although it is valid for the mean of a larger sample. Besides temperature fluctuations, the specific glacier geometry and variations in precipitation have to be taken into account for

the interpretation of the length fluctuations of an individual glacier. Hence, we use a coupled glacier mass balance–ice dynamical model to study the response of Glaciar Frías to climatic changes during the last four centuries.

In the next section, we describe the general setting of Glaciar Frías and the available information for driving and calibrating the glacier model. This model has two components: the first one calculating the surface mass balance from temperature and precipitation, and the second describing the ice-flow dynamics of the glacier. Section 3 gives a description of both components and an evaluation of the model performance. In Sect. 4, we discuss the characteristics of Glaciar Frías in its response to changes in climate. We then use the glacier model to extract the climatic information from the historical length record. Firstly, this is done directly by using dynamic calibration of the mass balance (Oerlemans, 1997a). Secondly, we force the glacier model with existing proxy climate records from this region (Villalba et al., 2003; Neukom et al., 2010, 2011). A comparison of the resulting modelled glacier length with the observed glacier fluctuations gives an indication of the accuracy of the existing climate reconstructions. To conclude, we study the behaviour of Glaciar Frías under the projected climate change of the 21st century.

## 2 Data

### 2.1 Study site

Glaciar Frías (41.15° S, 71.83° W) is located on the northeast face of Monte Tronador, a peak 3484 m high on the Chilean–Argentinean border in the north Patagonian Andes (Fig. 1a). The climate of the Tronador region is temperate maritime, with prevailing westerlies and large amounts of precipitation, predominantly in winter (Villalba et al., 1990; Brock et al., 2007). The Patagonian Andes form an effective north–south barrier to the westerlies. Hence, the region is characterized by a large west–east precipitation gradient, with over 2 m of precipitation on the western side and less than 1 m on the eastern side (Villalba et al., 2003).

Monte Tronador has several glaciers on the Chilean as well as on the Argentinean side. These glaciers have shown a general pattern of recession since the Little Ice Age (LIA) maximum, identified in this area between the 17th and the 19th centuries (Villalba et al., 1990; Masiokas et al., 2010). Glaciar Casa Pangué has retreated 1938 m in the period 1911–2000 (WGMS, 2008, updated; and earlier volumes), and the surface of its lower ablation area has thinned by  $2.3 \pm 0.6 \text{ m a}^{-1}$  on average between 1961 and 1998 (Bown and Rivera, 2007). Likewise, the regenerated portions of Glaciar Castaño Overo and the Glaciar Río Manso have retreated noticeably over the last decades (WGMS, 2008, updated; and earlier volumes; Masiokas et al., 2010). Recently, Ruiz et al. (2012) reconstructed the length fluctuations of Glaciar Esperanza Norte, 110 km south of Glaciar Frías.

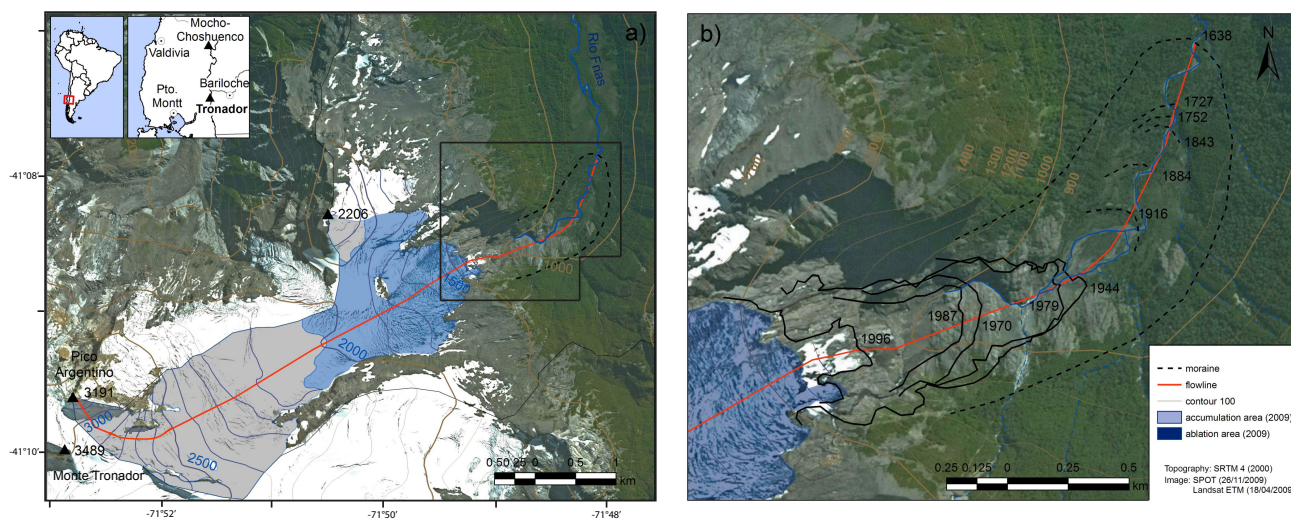


**Fig. 1.** (a) Topography of Glaciar Frías, flowing from the Argentinean summit on the northern slopes of Monte Tronador. The accumulation and ablation area of Glaciar Frías (2009) are indicated with grey and blue shading, respectively. The central flowline is given in red, and altitude in 100 m contour lines. The location of Monte Tronador is shown in the insets. (b) Close-up of the glacier forefield with the observed and reconstructed glacier terminus positions. For clarity, not all observations are included; see Table 1 for the complete length record.

The maximum extent of this glacier was dated to the mid-17th century. In addition, several moraines were dated during the 18th and 19th centuries. Glaciar Esperanza Norte experienced a large recession of more than 2 km in the 20th century, with a minor readvance in the 1970s.

The length records of Glaciar Esperanza Norte and Glaciar Frías are remarkably similar. Glaciar Frías has also substantially retreated over the 20th century (Fig. 1b). Between 1916 and 2009, the glacier terminus retreated 1.9 km. The fluctuations of Glaciar Frías have been reconstructed for the last four centuries from dendro-geomorphological, historical and field measurements (Villalba et al., 1990). Until a few decades ago, the tongue of Glaciar Frías was located well below the tree line. This made it possible to reconstruct the length variations back to 1639 through dendrochronological dating of moraines (Villalba et al., 1990). In addition, there exist historical sources (a 1856 etching depicting the Frías valley, which shows the tongue of Glaciar Frías in the background, Fonk, 1886, a 1936 photograph of the glacier terminus, Agostini, 1949) and annual field measurements from 1976 to 1985. For this study, the existing length record of Glaciar Frías has been extended using aerial photography and satellite images (Table 1, Fig. 1b). The entire record was revised by identifying the moraines dated by Villalba et al. (1990) on the 2009 SPOT satellite image, such that all length changes are measured consistently. The field measurements are connected to the record with the frontal position in 1979 taken from a Hexagon satellite image. At present, the length record of Glaciar Frías is one of the most detailed long records of the past millennium in South America (Masiokas et al., 2009). In addition, Glaciar Frías has no extensive debris cover, calving at the terminus, or surges. This makes the

length fluctuations of Glaciar Frías well suited for climate reconstruction.

Because of the diversity of methods used in the determination of the glacier length changes, the length record has a variety of uncertainties. The glacier outlines from satellite images and aerial photos (Table 1) have an exact date, and the uncertainty in derived glacier length is estimated to be 10–50 m, i.e. 2 pixels, to account for rectification and interpretation errors. The field measurements were carried out yearly at unspecified dates, and are considered to be accurate within 10 m. The dates of the historical sources are also well known, up to the year, but the spatial uncertainty can be large, especially for the 1856 etch (accuracy taken to be  $\pm 150$  m). The positions of the dated moraines are well known (within 50 m), but the dating has an uncertainty in the determined age of the trees and in the estimated time of seedling establishment (Luckman, 2000). Villalba et al. (1990) give an uncertainty of 20 yr for the dating in the Frías valley.

The geometry of Glaciar Frías has been derived from a 2009 SPOT 5 image (Table 1), in combination with the SRTM v.4 digital elevation model (DEM) from 2000. The voids in the data, which are common in SRTM, are interpolated in the current version of SRTM, and the vertical accuracy of the DEM is better than 9 m (Farr et al., 2007). Studies of DEM comparison suggest interpolation method provides a good means of filling the missing values, although some topographic detail is lost (Jarvis et al., 2004). In 2009, the glacier had an area of 6.54 km<sup>2</sup> and was 5.55 km long, flowing from 3190 m down to 1450 m on the northern slopes of Monte Tronador. The glacier surface is rather steep, with a mean slope of 0.32, but it has a more gentle slope around 2000 m (Fig. 2a). The glacier hypsometry is shown in Fig. 2c.

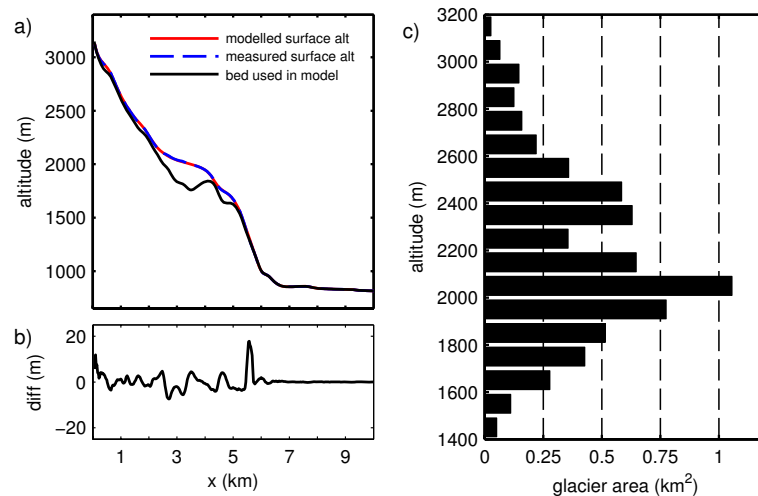


**Fig. 2.** (a) Surface altitude along the glacier flow line (dashed blue) from the DEM. For  $0 < x < 5.6$  km, the DEM gives the ice surface altitude instead of the bed altitude. Here, the bed profile (black) is determined with the ice flow model. The modelled glacier surface is shown in red. (b) Difference between modelled and observed surface altitude. The difference is less than 10 m except for  $5.6 < x < 5.7$  km, where there is ice in the model run (whereas in 2000 the terminus was at  $x \approx 5.6$  km). (c) Elevation distribution of the 2009 glacier area in 100 m intervals as derived from the 2000 DEM.

A large part of the area is in the 2000–2200 m range, with a much narrower accumulation area above 2600 m. The glacier tongue is relatively narrow, also when the glacier was larger in the past (Fig. 1).

In our dynamical model (Sect. 3.2), we use the central flowline and we parameterise the lateral glacier geometry with a trapezoidal cross section. The central flowline is determined from the DEM and corrected manually. The width of the valley floor and the slope of the valley walls are derived from 25 cross sections.

## 2.2 Meteorological and glacier mass balance data

Unfortunately, the glaciological and meteorological information available for the Glaciar Frías area is scarce. No mass balance measurements are available for Tronador glaciers, and meteorological records are either short, low resolution, or distant from the study site. Based on short-term precipitation measurements made in the late 1950s, Gallopin (1978) estimated that annual precipitation in the accumulation area of Monte Tronador is between 4.5 and 7 m w.e.

For two other glaciers in the Chilean Lake District, with a climate comparable to Glaciar Frías, glacier mass balances have been measured. Rivera et al. (2005) and Bown et al. (2007) describe glaciological mass balance measurements (stakes and snow density measurements) collected during the two hydrological years 2003/2004 and 2004/2005 on Glaciar Mocho, on the southeastern slopes of the Mocho-Choshuenco volcanic complex. This volcano has been inactive since 1864 and lies 130 km north of Glaciar Frías (Fig. 1). The equilibrium line altitude (ELA) of Glaciar Mocho lies between 1950 and 2000 m. The winter

balance at 2000 m varied between 2.9 and 4 m w.e.  $a^{-1}$ , and the annual mass balance varied between  $-0.88$  and 3.4 m w.e.  $a^{-1}$ . Furthermore, a large mass balance gradient of 0.015 m w.e.  $a^{-1} m^{-1}$  was measured. Brock et al. (2007) operated an automatic weather station (AWS) during several periods in 2004 and 2005 on the Pichillancahue-Turbio glacier on the active Volcán Villarrica, 190 km north of Glaciar Frías. Due to the volcanic activity of Volcán Villarrica, the mass balance of this glacier is strongly influenced by tephra covering the surface. Therefore, these measurements of the surface energy balance are not directly applicable to the mass balance of Glaciar Frías. However, Brock et al. (2007) present several results of interest for this study: they measured significant melt events at the ELA during the accumulation season caused by high air temperatures, and they confirm the high accumulation and melt rates found by Rivera et al. (2005) and Bown et al. (2007). In a reconstruction of the ELA of glaciers along the Andes of South America from a compilation of  $0^{\circ}C$  isotherm altitude and precipitation, Condom et al. (2007) give an ELA between 1800 and 2200 m for the region of Glaciar Frías. Carrasco et al. (2008) also report similar values from improvements of the relations used by Condom et al. (2007) for the southern Andes.

The meteorological stations nearest to Glaciar Frías with long, complete, temperature records are Bariloche at 55 km to the east and Puerto Montt at 100 km to the west (Fig. 1). At Puerto Montt, radio-sonde measurements are performed once or twice a day, but the record has a considerable amount of missing data. Long, complete precipitation records from sites close to Glaciar Frías are not available. The existing precipitation measurements show a very large precipitation gradient over the Andes (Villalba et al., 2003). The station of Punta

**Table 1.** Glacier length record of Glaciar Frías used in this study, including year of measurement (or reconstructed date of maximum extent), total length along the flowline (km), cumulative length change (m), method of observation (*moraine* indicates a moraine dated with dendrochronology; *historical* are historical sketches and photos; *field* denotes field measurements of terminus position; and *Landsat*, *Hexagon*, *SPOT* and *ASTER* are positions measured from satellite images), data source, and estimate of accuracy of the length measurement (m).

year	L (km)	dL (m)	type	source	accuracy (m)
1639	7.90	0	moraine	Villalba et al. (1990)	50
1727	7.63	-262	moraine	Villalba et al. (1990)	50
1752	7.58	-316	moraine	Villalba et al. (1990)	50
1843	7.53	-364	moraine	Villalba et al. (1990)	50
1856	7.50	-400	historical	Fonk (1886)	150
1884	7.35	-549	moraine	Villalba et al. (1990)	50
1916	7.14	-752	moraine	Villalba et al. (1990)	50
1936	6.77	-1125	historical	Agostini (1949)	20
1944	6.77	-1125	aerial	SHN	10
1970	6.36	-1534	aerial	IGM	10
1973	6.74	-1157	Landsat MSS	GLCF	120
1976	6.78	-1141	field	S. Rubulis	10
1977	6.77	-1121	field	S. Rubulis	10
1978	6.74	-1159	field	S. Rubulis	10
1979	6.71	-1181	field/Hexagon	S. Rubulis/EROS	10
1980	6.69	-1207	field	S. Rubulis	10
1981	6.61	-1231	field	S. Rubulis	10
1982	6.62	-1277	field	S. Rubulis	10
1983	6.55	-1343	field	S. Rubulis	10
1984	6.47	-1427	field	S. Rubulis	10
1985	6.44	-1453	field	S. Rubulis	10
1986	6.32	-1463	Landsat TM	GLCF	50
1987	6.29	-1495	Landsat TM	GLCF	50
1996	5.89	-1886	field	S. Rubulis	20
2003	5.56	-2607	ASTER	GLIMS	30
2007	5.73	-2444	Landsat ETM	CONAE	50
2009	5.55	-2617	SPOT	Spot image	10

SHN = Servicio de Hidrografía Naval, Argentina

IGM = Instituto Geográfico Nacional, Argentina

GLCF = Global Land Cover Facility, University of Maryland, USA

S. Rubulis = field measurements of S. Rubulis, reported in Villalba et al. (1990)

EROS = Earth Resources Observation and Science Center, US Geological Survey

GLIMS = Global Land Ice Measurements from Space

CONAE = Comisión Nacional de Actividades Espaciales, Argentina

Huano, located 35 km west of Glaciar Frías at 200 m altitude, has an average of  $3.2 \text{ m a}^{-1}$  over the 10 years of precipitation measurements in the period 1969–1980, whereas at Bariloche, on the eastern side of the Andes, an average annual precipitation of 0.88 m is measured over the period 1931–2009 (NOAA National Climatic Data Center, 2011; Peterson and Vose, 1997).

Because of the lack of nearby weather stations with long and detailed records, we use ERA-interim reanalysis data (1 January 1989–18 December 2010;  $0.75^\circ$  resolution) (Simmons et al., 2006) to force the mass balance model. The ERA-interim data are extended with ERA-40 reanalysis data (ECMWF Re-Analysis, 1 September 1957–1 September 2002;  $1.125^\circ$  resolution) for the period 1 January 1980–31 December 1988. Although ERA-40 is available from

1957, data for the mid and high latitudes on the Southern Hemisphere are not reliable in the presatellite era (Bromwich and Fogt, 2004). The spatial resolution of the ERA reanalysis data is too low to adequately resolve the local weather on an individual mountain. Therefore, we are limited to a mass balance that is based on the climatology of the reanalysis. We calculate monthly averages of temperature at 2000 m, the amplitude of the daily cycle, and the annual averaged lapse rate from the 6-hourly temperature values at the 4 grid points surrounding Glaciar Frías. The lapse rate and 2000 m temperature are derived from a linear fit through the pressure levels between 900 hPa and 500 hPa (10 levels for ERA-interim, 4 for ERA-40). The precipitation is calculated from the sum of convective and large-scale precipitation given at the surface level. For each month of the year,

the climatological averages over the 1980–2009 period are calculated for each grid point and bilinearly interpolated to the location of Glaciar Frías (Fig. 3).

The temperature climatologies at the four grid points are very similar, but the calculation of precipitation is more difficult. Because two of the four grid points used in the temperature calculation are located on the eastern side of the Andes, these give lower precipitation totals. As the glacier of our interest is on the water divide, where we expect the maximum precipitation, we only take the western grid points into account. Still, the ERA reanalysis precipitation of  $2.05 \text{ m a}^{-1}$  is much lower than that measured at Punta Huano station. This is probably due to the relatively low resolution of the ERA topography, as also the gradient in the ERA precipitation across the Andes is not as strong as derived from the measurements. For the input of the glacier mass balance model, described in the next section, we have increased the ERA precipitation with a factor 2.2, such that the modelled winter accumulation at 2000 m is in agreement with the measured winter accumulation of Glaciar Mocho. The relative distribution of the annual precipitation over the months in the ERA data is assumed to be correct.

### 2.3 Climate reconstructions for southern South America

For north Patagonia, several reconstructions of temperature (e.g. Villalba et al., 1997, 2003) and precipitation (e.g. Villalba et al., 1998; Lara et al., 2008; Boucher et al., 2011) exist. Neukom et al. (2010, 2011) have compiled a temperature and precipitation reconstruction for southern South America on a  $0.5^\circ \times 0.5^\circ$  grid from a selection of the available proxy records. In this study, we use the Neukom et al. (2010, 2011) and the Villalba et al. (2003) reconstructions to drive the glacier model, and then examine how well the observed glacier lengths are reproduced.

Neukom et al. (2011) provide gridded summer (DJF) and winter (JJA) temperature anomalies at yearly resolution for the periods 900–1995 and 1706–1995, respectively. These reconstructions were designed for analyses on sub-continental and continental scales, but we will examine to what extent they can be used to explain the observed local glacier fluctuations. As with the ERA reanalysis data, we use the values of the four grid points surrounding Glaciar Frías to compute the temperature anomalies with bilinear interpolation. Since the mass balance of Frías is sensitive to temperature perturbations in every month of the year (see Sect. 4.1), we apply the summer anomaly not only to the three summer months DJF, but to the summer half year November–April. Likewise, the winter anomaly is applied to May–October. In the period before 1706, when no winter temperatures are available, we apply the summer anomaly to the entire year. Winter and summer precipitation anomalies (Neukom et al., 2010) are available for the period 1590–1995 and 1498–1995, respectively. Like with temperature, the precipitation anomalies of

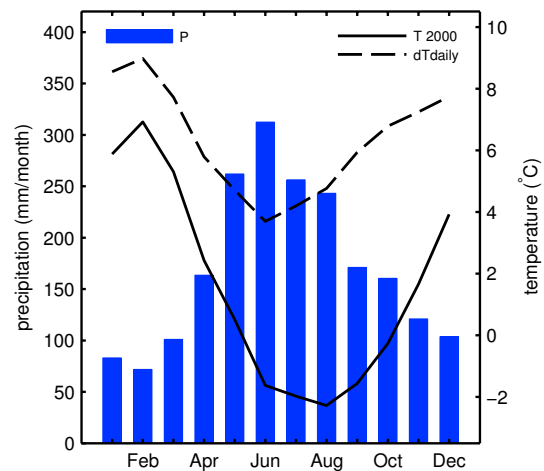


**Fig. 3.** 1980–2009 climatology of Glaciar Frías, from a combination of ERA-40 and ERA-interim data. Shown are the meteorological parameters needed for the mass balance model: monthly average temperature at 2000 m (black), amplitude of the daily cycle (dashed black), and average monthly sum of precipitation at 850 m (blue).

DJF are extended to the summer half year, and JJA precipitation anomalies to the winter half year, to get anomalies for every month of the year.

For additional comparison, we also drive the model with 1640–1987 tree-ring based annual temperature anomalies as reconstructed by Villalba et al. (2003) for the Monte Tronador region. The reconstructed temperature anomalies reflect the annual temperature anomalies (Villalba et al., 2003). These records are not used in the temperature reconstruction of Neukom et al. (2011); the two temperature reconstructions are independent. For precipitation we again use the Neukom et al. (2010) reconstruction. Annual average temperature anomalies of both reconstructions and precipitation anomalies of Neukom et al. (2010) are shown in Fig. 4.

## 3 Methods

### 3.1 Mass balance

The lack of mass balance and detailed meteorological measurements in the direct vicinity of Glaciar Frías makes it impossible to drive and validate a detailed surface energy balance model. In this study, a simple surface mass balance model is used to calculate the annual surface mass balance, following the approach of Oerlemans (2010), further extended in Giesen and Oerlemans (2012). The model is driven with monthly averaged temperatures and monthly precipitation totals of the ERA reanalysis (Sect. 2.2). A concise description of the model is given below; for details we refer to Giesen and Oerlemans (2012). An overview of the model parameters and their values is given in Table 2.

**Table 2.** Model parameter values of the surface mass balance model and the ice-dynamical model.

Parameter	Symbol	Value	Unit
Temperature lapse rate	$\gamma$	0.0048	$^{\circ}\text{C m}^{-1}$
Precipitation lapse rate	$p$	0.0015	$\text{m a}^{-1} \text{m}^{-1}$
Threshold temperature for snow	$T_{\text{snow}}$	1.5	$^{\circ}\text{C}$
Atmospheric transmissivity ( $\tau$ ) constant	$\tau_0$	0.55	–
Amplitude seasonal variation $\tau$	$A$	0.15	–
Phase shift $\tau$	$\delta p$	$0.55 \pi$	–
Water density	$\rho_w$	1000	$\text{kg m}^{-3}$
Ice density	$\rho_{\text{ice}}$	900	$\text{kg m}^{-3}$
Latent heat of melt	$L_f$	$3.34 \times 10^5$	$\text{J kg}^{-1}$
Fresh snow albedo	$\alpha_{\text{fr snow}}$	0.69–0.90	–
Firn albedo	$\alpha_{\text{firn}}$	0.53	–
Ice albedo	$\alpha_{\text{ice}}$	0.35	–
Albedo time-scale	$t^*$	21.9	days
Albedo depth-scale	$d^*$	0.001	m w.e.
Heat capacity of subsurface layer	$C$	$3.76 \times 10^6$	$\text{J m}^{-2} \text{ }^{\circ}\text{C}^{-1}$
Threshold temperature $\psi(T_a)$	$T_{\text{thresh}}$	0.44	$^{\circ}\text{C}$
Minimum $\psi(T_a)$	$\psi_{\text{min}}$	–30	$\text{W m}^{-2}$
Slope $\psi(T_a)$	$c_1$	9	$\text{W m}^{-2} \text{ }^{\circ}\text{C}^{-1}$
Sliding constant	$f_s$	$5.7 \times 10^{-20}$	$\text{Pa}^{-3} \text{ m}^2 \text{ s}^{-1}$
Deformation constant	$f_d$	$1.9 \times 10^{-24}$	$\text{Pa}^{-3} \text{ s}^{-1}$
Gravitation constant	$g$	9.81	$\text{m s}^{-2}$

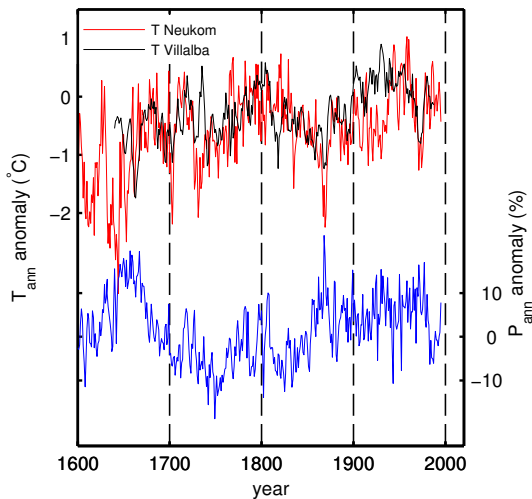


**Fig. 4.** Annual temperature anomaly from the Villalba et al. (2003) (black) and Neukom et al. (2011) (red) and annual relative precipitation anomaly from Neukom et al. (2010) (blue) w.r.t. the 1980–2009 mean. The annual anomalies from Neukom et al. (2010, 2011) are constructed from summer and winter anomalies as described in the text.

The annual surface mass balance at a certain point on the glacier is given by

$$b_{\text{ann}} = \int_{\text{year}} P_{\text{snow}} + (1 - r) \min \left( 0; -\frac{Q}{\rho_w L_f} \right) dt, \quad (1)$$

where  $P_{\text{snow}}$  (m w.e.) is the mass gained from solid precipitation and the mass loss is determined from the surface energy balance  $Q$ . Melt is assumed to occur when the surface energy balance is positive. Part  $r$  of the meltwater is allowed to refreeze in the snowpack. The constants  $\rho_w$  and  $L_f$  are the water density and latent heat of melt, respectively. The mass balance is calculated at hourly time steps.

Precipitation is assumed to increase linearly with altitude with lapse rate  $p$  (Table 2). Hourly precipitation is obtained by equally distributing the monthly total over all hourly time steps of the month. Temperature is determined from the monthly mean temperatures and an additional daily cycle, with a monthly amplitude. Both the precipitation and the temperature lapse rate are constant throughout the year. Precipitation that falls at air temperatures below  $1.5^{\circ}\text{C}$  is assumed to be solid  $P_{\text{snow}}$ .

Because humidity, cloudiness, and wind speed data are not available for the surface of Glaciar Frías, the energy available for melt is calculated from a simplified representation of the surface energy balance that only requires temperature and solid precipitation as input. The surface energy is divided into the net solar radiative flux and a second term,  $\psi(T_a)$ , that represents all other atmospheric fluxes as a function of air temperature only:

$$Q = (1 - \alpha) \tau S_{\text{in}} + \psi. \quad (2)$$

The net incoming short-wave radiation is calculated by multiplying the incoming solar radiation at the top of the

atmosphere on a plane by the mean slope and aspect of Glaciar Frías ( $S_{in}$ ), with the atmospheric transmissivity  $\tau$ .  $S_{in}$  is calculated from standard astronomical relations (e.g. Iqbal, 1983). The atmospheric transmissivity is higher in summer than in winter, and its seasonal cycle is expressed as

$$\tau = \tau_0 + A \sin\left(\frac{2\pi}{365}t + \delta p\right), \quad (3)$$

with constants  $\tau_0$ ,  $A$ , and  $\delta p$ , and time  $t$  expressed in days of the year. The constants are based on two years of measured incoming radiation at Glaciar Mocho (data kindly provided by M. Schaefer, CECS). Subsequently, the part of the incoming solar radiation that is reflected by the surface with albedo  $\alpha$  is subtracted. When no snow is present, we use a constant ice albedo  $\alpha_{ice}$ . After fresh snow has fallen,  $\alpha$  decreases exponentially in time from the fresh snow albedo  $\alpha_{fr\ snow}$  to the firm albedo  $\alpha_{firm}$ , with a time scale  $t^*$  (Oerlemans and Knap, 1998). For snowfall around the melting point,  $\alpha_{fr\ snow}$  is dependent on air temperature. For small snow depths,  $\alpha$  is a function of both the snow albedo and the ice albedo, according to a depth-scale  $d^*$  (Giesen and Oerlemans, 2010).

The remaining atmospheric fluxes (net long-wave radiation, latent and sensible heat) are parameterized by  $\psi$  as a function of air temperature only. The parameterization is based on in-situ measurements of these fluxes with automatic weather stations on several glaciers (Giesen and Oerlemans, 2012). A threshold temperature  $T_{thresh}$  is defined, below which  $\psi$  has the constant value  $\psi_{min}$  and above which  $\psi$  increases linearly with air temperature  $T_a$ .

$$\psi = \begin{cases} \psi_{min} & \text{for } T_a < T_{thresh} \\ \psi_{min} + c_1 T_a & \text{for } T_a \geq T_{thresh} \end{cases} \quad (4)$$

The best choice for the parameters  $T_{thresh}$ ,  $c$ , and  $\psi_{min}$  depends on the climatic setting of the glacier. The long-wave and turbulent fluxes depend on, besides temperature, the moisture content and cloud cover. Therefore, the model parameters that suit a maritime climate should be chosen to calculate the surface energy balance of Glaciar Frías. Here, we use values derived from surface energy balance measurements on maritime glaciers in Norway.

If snow is present, part of the meltwater that is formed when  $Q$  is positive is allowed to refreeze. Following Oerlemans (1991), this part  $r$  is dependent on the temperature of the subsurface layer  $T_{sub}$  ( $^{\circ}C$ ):

$$r = 1 - e^{T_{sub}}. \quad (5)$$

The refreezing of meltwater heats the snowpack, leading to a change in the subsurface temperature  $T_{sub}$ , calculated as

$$\frac{dT_{sub}}{dt} = \frac{rQ}{C}, \quad (6)$$

where  $C$  is the heat capacity of the subsurface layer, taken equivalent to a 2-m-thick layer of ice. At the end of the ablation season (the 30th of April),  $T_{sub}$  is reset to the annual

mean air temperature. If this temperature is higher than  $0^{\circ}C$ ,  $T_{sub}$  is set to  $0^{\circ}C$ , and no refreezing will occur. This means that, for the 1980–2009 climate, refreezing only occurs above 2350 m.

For the steady-state run with 1980–2009 climate, the mass balance model is run at 50 m intervals between 700 and 3400 m a.s.l. to calculate the climatic mass balance profile  $b_{ref}$  as a function of height. The dynamical model, described below, is forced with this profile, until a steady state is reached. When the reconstructed monthly precipitation and temperature anomalies are used as input for the glacier mass balance model, a mass balance profile is calculated for each year in the period covered by the reconstruction (1600–1995 for Neukom et al., 2011 and 1640–1987 for Villalba et al., 2003), again from 50 m intervals between 700 and 3400 m. This mass balance record is then used to force the dynamical model for the same period, after a spin-up time of 100 yr with the mean mass balance profile of the first 30 yr of the reconstruction.

In order to infer climatic information directly from the historical length record of Glaciar Frías, the mass balance history is reconstructed by dynamic calibration (Oerlemans, 1997a). In this method, it is assumed that at all times the mass balance profile  $b(z, t)$  can be described by an altitude-independent balance perturbation  $\delta b(t)$  added to the reference profile  $b_{ref}(z)$ :

$$b(z, t) = b_{ref}(z) + \delta b(t). \quad (7)$$

The mass balance profile from the 1980–2009 climate is taken as the reference profile  $b_{ref}$ . The values for  $\delta b$  are taken such that the difference between the modelled glacier length record and the observed glacier lengths is minimised. An optimised sequence of step functions is generally sufficient to describe  $\delta b$ . The model has a spin-up period of 100 yr with  $\delta b_{start}$ , such that the glacier has the steady-state length of the first observation when the record starts. The dynamical glacier model is run for the period of the observed length record, forced by the reconstructed mass balance history. If the dynamical model reproduces the observed lengths, the mass balance history is assumed to be correct.

### 3.2 Glacier dynamics

We use a one-dimensional flowline model to describe the ice dynamics. This model has been used earlier in studies of several other glaciers (e.g. Stroeven et al., 1989; Greuell, 1992; Oerlemans, 1997a,b), so here we only give a brief description. An overview of the variables is given in Table 3 (model constants are given in Table 2).

Starting from conservation of mass, we can define for each vertical cross-sectional area  $S$  along the flowline:

$$\frac{\partial S}{\partial t} = \frac{\partial(U S)}{\partial x} + w b, \quad (8)$$

where  $U$  is the vertical mean ice velocity of a cross section,  $w$  is the width at the glacier surface and  $b$  is the specific mass

**Table 3.** Model variables of the ice-dynamical model.

Variable	Symbol	Unit
Time	$t$	s
Distance along flowline	$x$	m
Area cross section	$S$	m <sup>2</sup>
Vertical mean ice velocity	$U$	m s <sup>-1</sup>
Specific mass balance	$b$	m w.e. s <sup>-1</sup>
Width glacier surface	$w$	m
Width glacier bed	$w_0$	m
Ice thickness	$H$	m
Surface altitude	$h$	m
Effective slope	$\lambda$	–

balance. We parameterise the cross section with a trapezoid. Thus, surface width  $w$  is given by

$$w = w_0 + \lambda H, \tag{9}$$

where  $H$  is the glacier thickness along the flowline,  $w_0$  is the basal glacier width, and  $\lambda$  is the effective slope of the valley wall. The area of the cross section  $S$  is given by

$$S = H \left( w_0 + \frac{1}{2} \lambda H \right). \tag{10}$$

Combining these three equations gives the time evolution of the ice thickness:

$$\frac{\partial H}{\partial t} = \frac{-1}{w_0 + \lambda H} \frac{\partial}{\partial x} \left\{ H U \left( w_0 + \frac{1}{2} \lambda H \right) \right\} + b. \tag{11}$$

We assume the glacier is entirely temperate and use the shallow ice approximation (SIA), such that the mean vertical ice velocity is entirely determined by the local driving stress  $\sigma$ . As suggested by Budd et al. (1979), we separate the vertical mean ice velocity in a component due to sliding and a component due to ice deformation:

$$U = U_d + U_s = f_d H \sigma^3 + f_s \frac{\sigma^3}{H}, \tag{12}$$

with  $\sigma$  given by the ice thickness  $H$  and surface slope  $\frac{\partial h}{\partial x}$  ( $h$  is the surface altitude):

$$\sigma = -\rho_{ice} g H \frac{\partial h}{\partial x}. \tag{13}$$

The values for the constants of deformation  $f_d$  and sliding  $f_s$  are taken from Budd et al. (1979) (Table 2). Substituting this expression for  $U$  into Eq. (11) gives the expression for the evolution of the ice thickness:

$$\frac{\partial H}{\partial t} = \frac{-1}{w_0 + \lambda H} \frac{\partial}{\partial x} \left\{ D \frac{\partial h}{\partial x} \right\} + b, \tag{14}$$

with  $D$ :

$$D = \left( w_0 + \frac{1}{2} \lambda H \right) \rho_{ice}^3 g^3 H^3 \left\{ f_d H^2 \left( \frac{\partial h}{\partial x} \right)^2 + f_s \left( \frac{\partial h}{\partial x} \right)^2 \right\}. \tag{15}$$

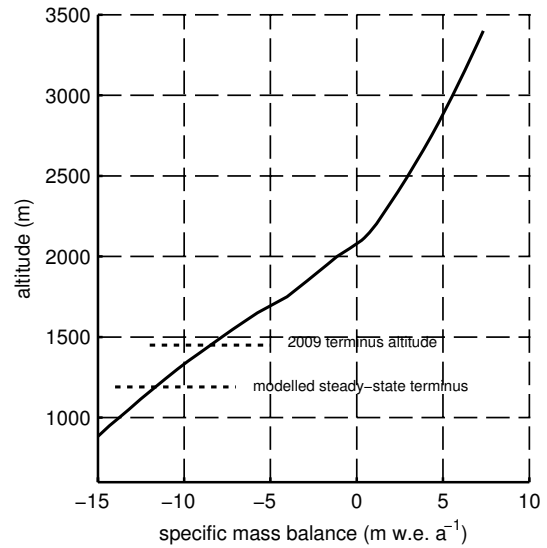


**Fig. 5.** Mass balance profile  $b_{ref}(z)$  calculated from 1980–2009 average forcing. NB: the profile is given for the entire model domain; the terminus is at 1450 m in 2009 (glacier length = 5550 m); the modelled steady-state terminus is at 1200 m altitude (glacier length = 5725 m).

Equation (14) is solved on a staggered grid, with a grid size of 25 m. Time integration is done with a forward explicit scheme, in time steps of 0.00025 yr (approx. 2 h). The length of the glacier is determined by the last grid point with non-zero ice thickness. The specific mass balance  $b$  is a function of surface altitude  $h$  and taken from the balance profile calculated with the mass balance model. For time-dependent simulations,  $b$  is recalculated every year.

### 3.3 Model calibration and validation

The climatological conditions of the period 1980–2009 are used as input for the mass balance model to calculate  $b_{ref}$  (Fig. 5). The calculated profile is almost linear below the ELA at 2090 m, and the gradient becomes smaller for higher elevations. This is in line with mass balance profiles observed elsewhere (e.g. Andreassen et al., 2005). The calculated mass balance gradient of 0.012 m w.e. m<sup>-1</sup> a<sup>-1</sup> is large, but smaller than measured at Glaciar Mocho. This could be caused by the less pronounced seasonality in the precipitation at the higher latitude of Glaciar Frías. The calculated ELA at Glaciar Frías is a bit higher than the ELA at Glaciar Mocho. This is reasonable, as the Glaciar Frías flows to the north-east and thus receives more incoming short-wave radiation than Glaciar Mocho, which flows towards the south-east. For a selected number of altitudes, the evolution of the cumulative mass balance throughout the hydrological year is shown in Fig. 6. The winter accumulation at 2000 m is 3.9 m w.e., but this all melts during the ablation season. The winter accumulation is in line with the accumulation at Glaciar Mocho. The annual

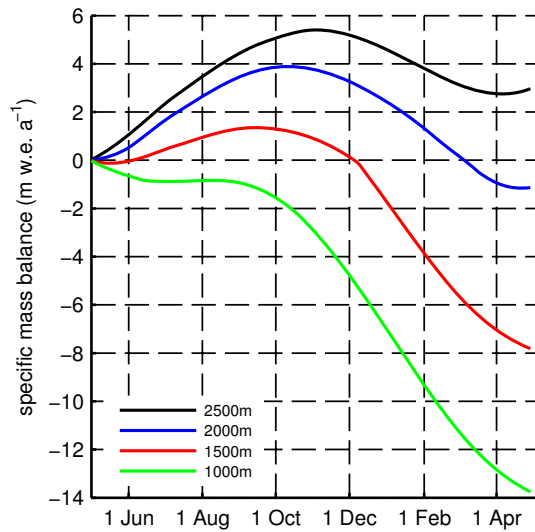


**Fig. 6.** Temporal evolution of the annual cumulative mass balance, shown in Fig. 5, at selected altitudes. The time evolution is shown during one mass balance year, which starts on 1 May and ends on 30 April.

precipitation at 2000 m that is needed for this amount of accumulation is 8.2 m w.e., which is at the high end of the observations of Gallopin (1978). As shown by the mass balance at 2500 m, ablation is still substantial above the equilibrium line, but this is outpaced by the accumulation. The model shows that at 1000 m there is hardly any accumulation, so in the 1980–2009 climate the glacier tongue would sustain year-round melting when it reaches the bottom of the Frías valley.

The topography of the glacier bed of Glaciar Frías is unknown, except for that part of the valley that is currently deglaciated. The bed topography of the part that is covered by ice is derived from the model (Sect. 3.2) forced with  $b_{\text{ref}}$  (Fig. 5). Following an iterative procedure, the bed altitude along the flow line and the glacier width at the bed are adjusted, such that the modelled surface width and altitude in equilibrium state match the observed surface width and surface altitude along the flow line. The observed surface altitude is that of a glacier in retreat, rather than in equilibrium, which could introduce an error in the reconstructed bed topography. However, model experiments show that the surface altitude of an equilibrium state hardly differs from the surface altitude of retreating Glaciar Frías with the same glacier length (difference is less than 5 m); hence, this error is negligible. The bed profile that reproduces the 2000 surface best (Fig. 2a) has an overdeepening around  $x = 3500$  m, followed by a bump that is at the same location as the ridge that is currently emerging from the ice at ca. 1800 m (Fig. 1).

If we force the ice-dynamical model with  $b_{\text{ref}}$  and the reconstructed bed topography, the calculated equilibrium glacier length is 5725 m. This is within the range of the observed glacier lengths in this period (cf. Fig. 10, Table 1),

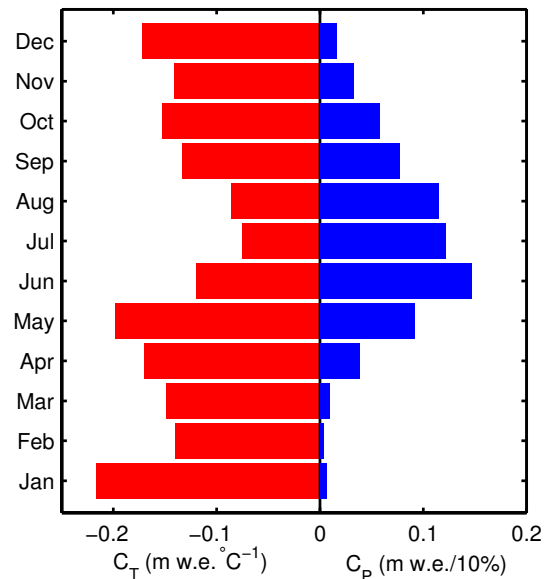


**Fig. 7.** Seasonal sensitivity characteristic, showing the sensitivity of the mass balance to changes in temperature ( $C_T$ ) and precipitation ( $C_P$ ) in a specific month. Changes in precipitation are relative, shown is the change in mass balance after a 10% change in monthly precipitation. Mass balance is calculated for the glacier geometry of the modelled equilibrium state with  $b_{\text{ref}}$ .

indicating that the calculated mass balance is fairly accurate. However, because no measurements of the individual components of the energy budget are available, compensating errors cannot be excluded.

## 4 Results and discussion

### 4.1 Sensitivity and response time of Glaciar Frías

Before using the coupled mass balance–glacier model for climate reconstruction, we examine the sensitivities of Glaciar Frías to climatic change. In Fig. 7, the seasonal sensitivity characteristic (SSC, Oerlemans and Reichert, 2000) of the mass balance of Glaciar Frías in equilibrium state is shown. The SSC consists of 24 numbers that give the sensitivity of the annual mass balance to monthly perturbations in precipitation and temperature. The temperature sensitivities indicate that Glaciar Frías is in a highly maritime climate. The SSC values are large and the mass balance is sensitive to temperature changes in every month of the year. Although the mass balance is more sensitive to changes in summer temperature than to changes in winter temperature, temperature anomalies in the winter season lead to significant changes in the mass balance. Furthermore, variations in winter precipitation are more important for the mass balance than variations in summer precipitation. Most of the precipitation falls in winter, and summer precipitation falls as rain on a large part of the glacier.

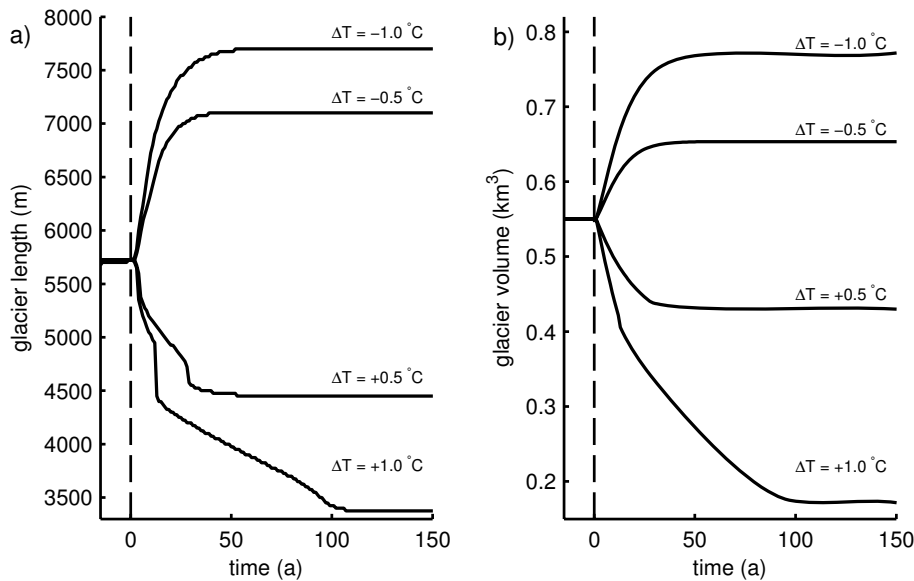


**Fig. 8.** (a) Length and (b) volumes changes of Glaciar Frías after perturbation of the 1980–2009 climate with  $\Delta T = +1.0, +0.5, -0.5$  and  $-1.0\text{ }^{\circ}\text{C}$  at  $t = 0$ . It shows the response of Glaciar Frías to perturbations in climate. For  $\Delta T = +1\text{ }^{\circ}\text{C}$ , the glacier retreats over the overdeepening in the bed, which causes a drastic decrease in both volume and length.

We calculate the e-folding response time and climate sensitivity of the glacier in equilibrium state by imposing a step-wise perturbation in the climatic forcing that is kept constant until the glacier has reached a new equilibrium (no changes in length and volume for a period of 50 yr at least). The climate sensitivity indicates the difference between the two equilibria. The response time is a measure for the time needed to reach the new equilibrium, defined as the time needed to reach  $1 - e^{-1}$  ( $\approx 0.63$ ) of the final change. As the mass balance is sensitive to temperature change in all months of the year, the perturbations consist of changes in the annual mean temperature. Examples of the response to changes of  $-1.0, -0.5, 0.5$  and  $1.0\text{ }^{\circ}\text{C}$  are shown in Fig. 8 for both glacier length and glacier volume. Glaciar Frías has a response time of 15 yr. This is short compared with other alpine glaciers (cf. Jóhannesson et al., 1989; Greuell, 1992; Oerlemans, 1997a,b; Brugger, 2007; Laumann and Nesje, 2009), indicating that Glaciar Frías reacts rather directly to changes in climate. The climate sensitivity depends on the perturbation. The climate sensitivity in glacier length varies between  $-750$  and  $-4875\text{ m }^{\circ}\text{C}^{-1}$  calculated from annual temperature anomalies in steps of  $0.1\text{ }^{\circ}\text{C}$  between  $-2$  and  $2\text{ }^{\circ}\text{C}$  (Fig. 9). The large range is caused by the irregular glacier geometry. It implies that length fluctuations of the same magnitude are not necessarily due to climate changes of the same magnitude: the change in forcing needed for a retreat from a glacier length of 9 to 8 km is more than twice as large as for a retreat from 6 to 5 km. The climate sensitivity is very high for the glacier in its 1980–2009 climate steady state. The good agreement between the modelled length and the observed length in this period is a strong indication the modelled mass

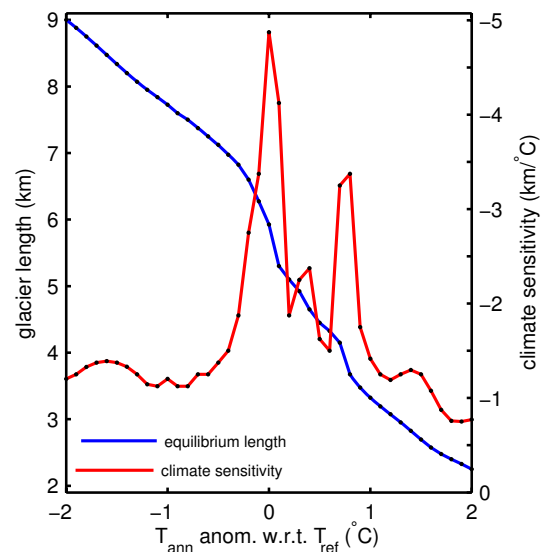


**Fig. 9.** Equilibrium length (blue, left scale) and climate sensitivity (red, right scale) of Glaciar Frías as a function of annual temperature anomaly w.r.t. the 1980–2009 mean. Equilibrium lengths (and therefore also climate sensitivities) are calculated for each  $0.1\text{ }^{\circ}\text{C}$  step in annual temperature anomaly (black dots).

balance is reasonable. Small changes in the reference mass balance  $b_{\text{ref}}$  would lead to relatively large length changes, such that the glacier length is a good constraint for the calculated mass balance.

## 4.2 Historical fluctuations

### 4.2.1 Climatic information from dynamic calibration

As shown in Fig. 10, the observed length record can be reproduced using dynamic calibration of the mass balance profile with a sequence of 13 step functions. To explain the maximum glacier length in 1639, the mass balance profile must have been  $1.7 \text{ m w.e. a}^{-1}$  more positive than the 1980–2009 mean profile. This maximum of  $\delta b$  is followed by a slight decline over the following two centuries, until the mass balance makes a significant drop at the end of the 19th century. In the 20th century, more length observations are available and thus the reconstructed  $\delta b$  then shows more fluctuations. The most striking fluctuation is around 1970, prior to the significant and well-documented re-advance of the glacier that culminated in 1977. Overall, there is a negative trend in the mass balance over the 20th century of  $-0.0079 \text{ m w.e. a}^{-2}$ . The current retreat is best explained by  $\delta b = -0.25 \text{ m w.e. a}^{-1}$  in the period 2001–2009. Hence, the glacier retreat over the entire period of the length record, 1639–2009, is best explained by a decrease in  $\delta b$  of  $1.95 \text{ m w.e. a}^{-1}$ .

Changes in the mass balance are in general due to changes in both precipitation and temperature. Although the influence of these two climate components cannot be disentangled from the mass balance reconstruction, it is possible to give a quantitative indication of the change in temperature or precipitation needed to arrive at the reconstructed mass balance profile to changes in annual temperature and precipitation is determined based on least squares fit of the mass balance profiles calculated with the temperature perturbations of  $\pm 0.5$  and  $\pm 1^\circ \text{C}$  and precipitation perturbations of  $\pm 10$  and  $\pm 20\%$ . The mass balance sensitivity to changes in temperature is  $-1.59 \text{ m w.e. a}^{-1} \text{ }^\circ \text{C}^{-1}$ , and  $0.58 \text{ m w.e. a}^{-1}$  per 10% increase in precipitation. The observed retreat of Glaciar Frías over the period 1639–2009 is thus best explained by a temperature increase of  $1.2^\circ \text{C}$ , or a precipitation decrease of 34% (meaning that the precipitation in the 17th century must have been 134% of present-day precipitation). Or, most likely, the observed glacier retreat is a combination of both. The 30 yr average in precipitation reconstructed by Neukom et al. (2010) decreased by 10% from the maximum in the period 1645–1674 to the period 1966–1995.

### 4.2.2 Forcing the glacier model with climate reconstructions

Instead of deriving a mass balance reconstruction based on dynamical calibration, we can also calculate the historical mass balance using the temperature and precipitation records based on other proxy reconstructions. In this way the observed glacier length can serve as a constraint on the proxy-based climate reconstructions. This could in addition provide information on the relative contributions of

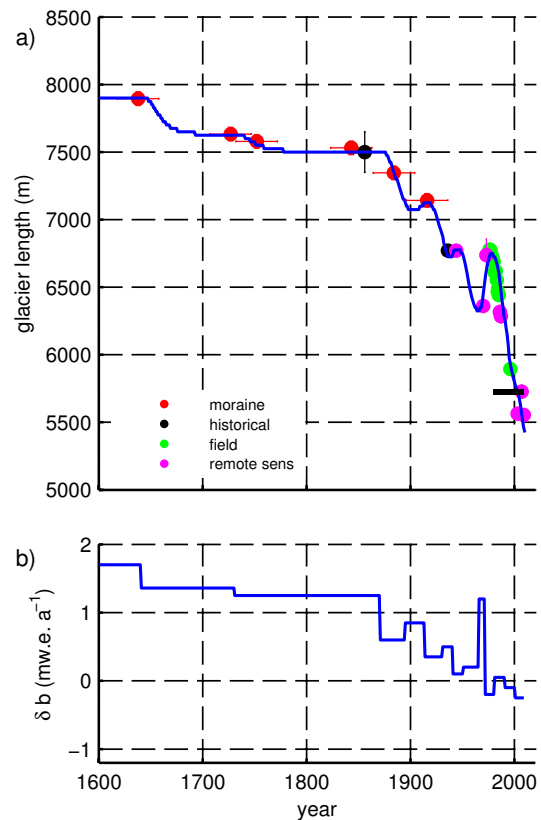


**Fig. 10.** (a) Observed glacier length of Frías (dots); colours indicate the type of observation (cf. Table 1); bars indicate the uncertainty in both time (dated moraines) and length (most of the times smaller than the dots); modelled equilibrium length for the 1980–2009 climate (horizontal black line); and modelled glacier length reconstructed with dynamical calibration (blue). (b) Mass balance perturbations  $\delta b$  that reproduce the observed glacier length.

fluctuations in precipitation and temperature to the glacier length changes. We force the glacier model with the reconstructions of Neukom et al. (2010, 2011) and Villalba et al. (2003). The calculated glacier length for the period 1600–1995 and 1640–1987, respectively, is shown together with the observed glacier length in Fig. 11a.

We first focus on the results calculated from the Neukom et al. (2010, 2011) reconstructions. The modelled length is promising in a qualitative sense: maximum extents before 1800, in 1884 and in 1916 are reproduced (although the timing of the maximum extents in the mid-17th century and in 1916 does not fall within the uncertainty margins of the dating of the moraines) together with the large retreat between 1880 and 1960, and the re-advance in the 1970s that is followed by the retreat that continues up to present day. However, the modelled glacier lengths do not exactly match the observations. The length variations in the 20th century are too large: the modelled glacier length in 1940 is 500 m larger than the observed length, while in 1970 it is 700 m shorter than observed, and the subsequent re-advance is again larger

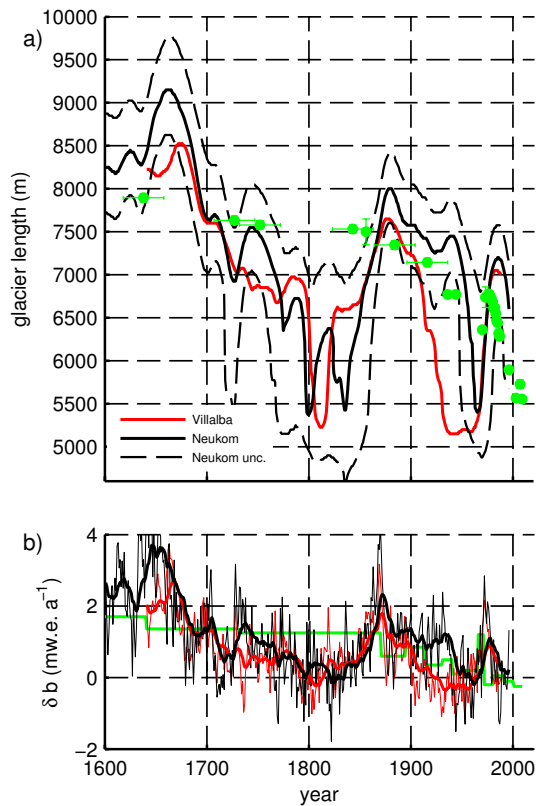


**Fig. 11.** Results of the model forced with the available precipitation (Neukom et al., 2010) and temperature (Neukom et al., 2011; Villalba et al., 2003) reconstructions. **(a)** Glacier length for the period 1600–1995 based on Neukom et al. (2011, 2010) (black), with upper and lower estimate (dashed black) indicating the uncertainty; Villalba et al. (2003) temperature, Neukom et al. (2010) precipitation (red); observations (green dots), with uncertainty intervals. **(b)**  $\delta b$  calculated from the annual mass balance profiles from the reconstructions by Neukom et al. (black), Villalba et al. (red), with 21-yr exponential smoothing, and  $\delta b$  obtained from dynamical calibration (green) (cf. Fig. 10).

than observed. The advance in the beginning of the 19th century is too small to reach the 1843 moraine, and the maximum extent in the 17th century is about 1.5 km too large. Only the 1727 and 1756 moraines are well reproduced by the modelled glacier length record.

The differences can to a large extent be explained by the uncertainties in the climate reconstructions. Using the decadal-scale uncertainties in the reconstructions of Neukom et al. (2010, 2011), we have estimated upper and lower limits for the modelled glacier length (dashed black lines in Fig. 11a). For the upper limit, we calculated maximum mass balance from the precipitation plus 1 standard error (SE) uncertainty and the temperature minus the 1 SE uncertainty. Likewise, we calculated the lower limit in modelled glacier length from the minimal precipitation and maximal temperatures within the 1 SE uncertainty margin. The uncertainty

in the reconstruction is fairly large, when translated into glacier length. The very large uncertainty range when the modelled glacier length is between 5000–7000 m is due to the larger climate sensitivity of the glacier in this range, not to a larger uncertainty in the reconstructions during these periods (cf. Fig. 9). Almost all glacier length observations fall within the range that is derived from uncertainty in the prescribed forcing. Only the constraints set by the maximum glacier length in the 1600–2009 period, as determined by the 1639 moraine, and the length measurements in 1843, 1936 and 1944 are not met.

With the Villalba et al. (2003) reconstruction as temperature forcing, the modelled glacier length is comparable to the previous reconstruction (Fig. 11a). Again, the modelled length qualitatively shows the same characteristics as the observed record, but the reconstruction fails to reproduce the length observations on more or less the same points in time as the reconstruction forced with the Neukom et al. (2011) temperature anomalies. However, in this second reconstruction the maximum extent is smaller, more in line with the observations (but timed later). And, in contradiction to the other reconstruction, the glacier extent is much smaller than observed throughout the entire first half of the 20th century.

We have calculated  $\delta b$  from the mass balance profiles of both reconstructions (Fig. 11b), to compare the differences in mass balance profiles between the results of the dynamical calibration and those obtained when the model is forced with reconstructed temperature and precipitation anomalies from north Patagonia. As the calibrated mass balance record only reproduces the observations in the simplest way, the mass balance based on the reconstructed temperature and precipitation cannot be expected to be identical. The glacier has likely experienced unobserved retreat in the periods between two maximum stands that are indicated by the moraines. With this in mind, still three discrepancies between the observed and modelled glacier lengths can be identified: (i) the  $\delta b$  based on Neukom et al. (2011) is more than  $1 \text{ m.w.e. a}^{-1}$  more positive in the period 1640–1660. (ii) Both reconstruction-based  $\delta b$ s are too low to reproduce the observed length in 1843. An increase of  $1.2 \text{ m.w.e. a}^{-1}$  in  $\delta b$  over the period 1800–1840 would reproduce the local maximum in glacier length in agreement with the 1843 moraine. (iii) There is a striking difference between the two reconstruction-based mass balances in the first half of the 20th century. The Neukom et al. (2011) reconstruction results in a too high mass balance with a too large glacier extent, while the Villalba et al. (2003) gives a much lower  $\delta b$ , which results in a too small glacier extent during this period.

The Neukom et al. (2010, 2011) climate reconstructions do not provide a complete record for the period covered by the length record. Prior to 1706, we used summer anomalies for the entire year. Forcing the glacier model with the summer temperature anomaly applied to all months of the year over the entire period 1600–1995 results in a similar modelled glacier length (Fig. 12). However, substantial differences can

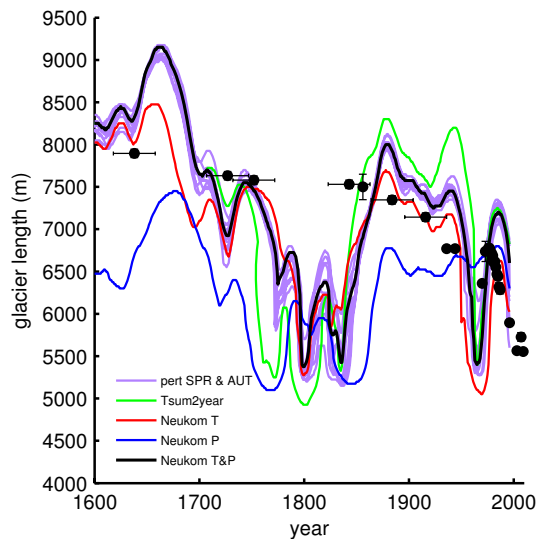


**Fig. 12.** Sensitivity of the modelled glacier length forced with Neukom et al. (2010, 2011) (black, cf. Fig. 11) to random perturbations added to spring and autumn temperature and precipitation (15 purple lines); using summer temperature anomaly as a proxy for annual temperature anomaly (green); only temperature anomalies, keeping the precipitation constant at the 1980–2009 level (red); forced with only precipitation anomalies, keeping temperature constant (blue). Observed glacier lengths are shown as black dots.

occur. Therefore, the modelled glacier lengths prior to 1720 (accounting for the response time) should be interpreted with care. Furthermore, the reconstructions only provide summer and winter anomalies for both temperature and precipitation that were used to derive values for the spring and autumn anomalies. To examine the sensitivity of the modelled glacier length to these assumptions, random perturbations are added to spring and autumn temperatures, as well as winter temperatures prior to 1706. The random perturbations, different for each season and year, are drawn from a normal distribution with the same standard deviation as the climate reconstruction time series. The model is forced with 15 different perturbed forcing series over the period 1600–1995. The spread in the 15-member ensemble is small in comparison with the uncertainty in the reconstructions (cf. Fig. 11) leading to the conclusion that only a systematic difference between spring/autumn temperatures and the summer/winter anomalies could lead to a significant difference in modelled glacier length. We have also calculated the length record from perturbations in temperature only, leaving the precipitation constant at the 1980–2009 mean. The resulting length record closely resembles the length record of the model run with perturbations in both temperature and precipitation. Likewise, the model is run forced with precipitation fluctuations only. The modelled length fluctuations are much smaller than modelled from the complete forcing. This indicates that the fluctuations in precipitation are in general of minor importance for the observed glacier fluctuations over the last four

centuries. Only in the mid-17th century, a positive precipitation anomaly significantly contributed to the glacier advance, accounting for an additional advance of 0.7 km (Fig. 12).

As the past glacier fluctuations appear to be mainly temperature driven, we express the differences between observations and modelled glacier length from the climate reconstructions in terms of temperature anomaly. It is difficult to draw firm conclusions for the period before 1706, as the uncertainties in the reconstructed mass balance are large due to the missing winter temperatures. If the summer anomaly is applicable to the annual anomaly, the best estimate of the reconstructed temperature of Neukom et al. (2011) for the middle of the 17th century is in the order of 0.7–1.0 °C too low. In the Neukom et al. (2011) reconstruction, the 1630–1659 average (summer!) temperature is 1.5 °C lower than the 1966–1995 average. In addition, the 1645–1674 precipitation is 10% higher than the 1966–1995 average. Also the temperature reconstruction of Villalba et al. (2003) gives a larger glacier length than the observed maximum extent. In addition the timing of the advance deviates from the dating of the moraine, but it should be noted that the Villalba et al. (2003) reconstruction does not start until 1640. The Villalba et al. (2003) 1640–1669 average temperature is 0.6 °C lower than the 1956–1985 average. This difference is smaller than in the Neukom et al. (2011) reconstruction, which has a temperature increase of 1.25 °C over the same period. Both reconstructions give too high temperatures around 1800. According to the modelled glacier length, the best estimate of the temperature anomaly should be 0.7 °C lower in the period 1800–1840. The overestimate of early 19th century temperature in the climate reconstructions is supported by the 1795, 1807, and 1830 moraines of Glaciar Esperanza Norte (Ruiz et al., 2012). The disagreement between the two reconstructions in the first half of the 20th century is remarkable, as for both reconstructions this period is part of the calibration period. The mass balance obtained from the dynamical calibration suggests that, for this period, the mean of the two temperature reconstructions would explain the observed glacier length.

The mismatch between glacier length modelled with the climate reconstructions and the observations could be an indication that the long-term variability in the reconstructions is too large: the mid-17th century too cold and the period around 1800 too warm. An alternative explanation is that the modelled glacier sensitivity to the climatic forcing is too large. The length record could be smoother if the glacier response is reduced by changing the ice dynamics. However, adjusting the sliding and deformation velocities of the glacier by choosing different parameter values for  $f_d$  and  $f_s$  (Eq. 12, Table 2) does not improve the modelled length record. Also the parameter choice in the mass balance model, where especially the parametrisation of  $\psi$  is uncertain, cannot explain the overestimated variations. Variation of these parameters leads to a more positive, or negative, mass balance for the entire period of reconstruction. Other parameter values thus

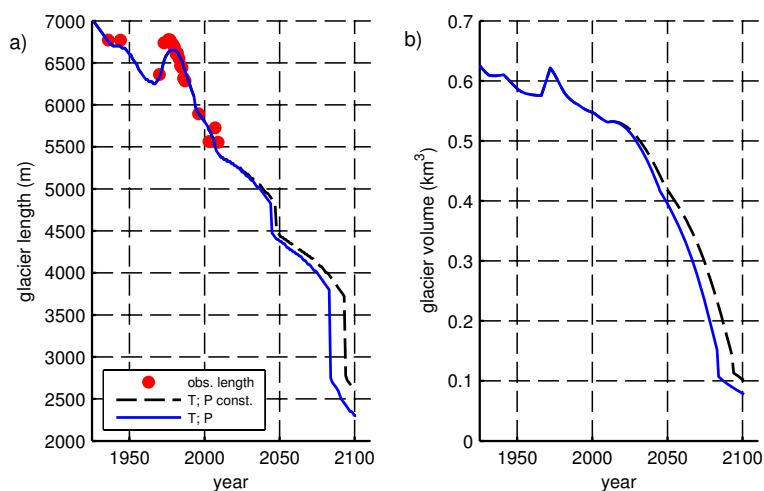


**Fig. 13.** Modelled (a) glacier length and (b) glacier volume of Glaciar Frías for the period 1925–2100. Glacier length and volume for the period 1925–2009 are calculated from the reconstructed mass balance profiles; for 2010–2100 the mass balance is calculated from the future scenario. The full scenario (increase in  $T$  of  $2^{\circ}\text{C}$  and decrease in  $P$  of 10 % over the 21st century) is shown in blue. The length and volume change with precipitation kept at the 1980–2009 level are given in dashed black. In (a) also glacier length observations are included (red dots).

lead to a constantly larger or smaller glacier, not to smaller or larger length fluctuations. To reduce the uncertainties in the glacier model, mass balance measurements and meteorological observations on Glaciar Frías are needed, such that the different components in the mass balance model as well as the model input can be validated.

### 4.3 Future of Glaciar Frías

Regional climate projections for South America predict a warming trend and decrease in precipitation over the next century for north Patagonia (Vera et al., 2006; Christensen et al., 2007). According to the IPCC A1B scenario, the annual precipitation will have decreased 15 % by the end of the 21st century, compared to the 1980–1999 average. The projected decrease for the summer (DJF) months is stronger than for the winter (JJA) months, with decreases in precipitation of 30 % and 5–10 %, respectively. For the period 2080–2099, annual mean temperature is projected to be  $2^{\circ}\text{C}$  higher than in the reference period 1980–1999. Again, the changes in summer ( $+2.5^{\circ}\text{C}$ ) are stronger than in winter ( $+1.5^{\circ}\text{C}$ ).

Figure 13 shows the future response of Glaciar Frías to the projected changes in north Patagonian climate. For simplicity, the coupled model was forced with a linear increase in annual temperature and a linear decrease in annual precipitation, such that in 2100 the annual temperature is  $2^{\circ}\text{C}$  higher than the 1980–2009 average, and annual precipitation has decreased 10 % in 2100. Based on this scenario, the glacier will retreat 3400 m to a length of 2175 m in 2100, and the terminus will retreat to an elevation of 2150 m. This projected retreat in length is larger than the retreat since the maximum stand in 1639. In terms of volume, the shrinkage is even more

pronounced: the glacier is projected to lose more than 80 % of its volume during the 21st century. This projected glacier retreat is not exceptional. Similar retreats are found in other model studies of glaciers in different parts of the world (e.g. Oerlemans et al., 1998; Adhikari and Huybrechts, 2009). A simple sensitivity test, in which the precipitation is kept at the 1980–2009 level (dashed black in Fig. 13), shows that the glacier retreat is mainly due to the increase in temperature. The extra precipitation slows down the retreat, but the eventual mass loss is very similar.

## 5 Conclusions

In this study we present a model for Glaciar Frías in the north Patagonian Andes of Argentina that has a length record spanning the period 1639–2009. Given the lack of detailed meteorological information near Glaciar Frías, we forced a simplified surface-energy balance model with climatological monthly temperature and precipitation values derived from ERA reanalysis. The results provided interesting new information regarding the climate sensitivity of this glacier and offered for the first time in Patagonia the possibility of comparing modelled glacier mass balance changes with those obtained from independent, proxy-based climate reconstructions.

Glaciar Frías is located in a temperate maritime climate. It is very sensitive to temperature changes and to a lesser extent sensitive to variations in precipitation, mainly to changes in winter precipitation. Glaciar Frías has a response time of only 15 yr, and therefore follows fluctuations in climate quite closely. The mass balance calculated with 1980–2009 climatology corresponds well with the little information that

is available in the north Patagonian Andes. The 1980–2009 equilibrium length is within the range expected from the glacier length observations.

The reconstructed mass balance history indicates that the overall retreat of Glaciar Frías during the period 1639–2009 can be best explained by a decrease of  $1.95 \text{ m w.e. a}^{-1}$  of the specific mass balance profile. This change in climatic conditions can be caused by an increase in temperature as well as, or in combination with, a decrease in precipitation. If it would only be attributed to changing precipitation, the precipitation in the mid-17th century must have been 134 % of the 1980–2009 average. If attributed to temperature, the mass balance decrease implies a temperature increase of  $1.2^\circ\text{C}$ . Only a minor warming/drying is needed to explain the difference in glacier length between the maximum LIA extent in 1639 and the mid-19th century. At the end of the 19th century, mass balance dropped substantially and continued to decrease in the 20th century with some fluctuations, of which the most striking was around 1970.

Driving the glacier model with independently reconstructed temperature and precipitation shows that the fluctuations of Glaciar Frías over the last four centuries were predominantly temperature-driven. In a comparison between modelled and observed glacier length fluctuations, existing proxy-based reconstructions of north Patagonian precipitation and temperature seem to represent the interdecadal variability well. The glacier model forced with these reconstructions produces glacier advances and retreats that in timing agree well with the dated moraines and observations. However, in quantitative sense, the reconstructed temperature and precipitation anomalies have a relatively high level of uncertainty. This is reflected in the large range of possible glacier lengths. In order to explain the observed length of Glaciar Frías, temperature around 1800 must have been lower than the best estimate of the reconstructed temperatures by Neukom et al. (2011) and Villalba et al. (2003). Lowering the temperatures with  $0.7^\circ\text{C}$  between 1800 and 1840 would produce a maximum extent that is in agreement with the 1843 moraine. The uncertainty in these results might be substantial, due to uncertainties in the climate reconstructions and in the glacier model, but are difficult to quantify.

Following the IPCC A1B scenario for north Patagonia, Glaciar Frías is projected to continue its rapid retreat in the near future. By 2100, the glacier will likely have lost more than 80 % of its present-day volume and the terminus will have retreated high up the Monte Tronador. Like with the past fluctuations, this expected retreat is mostly due to the projected increase in temperature.

*Acknowledgements.* We thank R. Neukom and R. Villalba for kindly providing their climate reconstructions, E. Betman for processing the Puerto Montt radio sonde data, M. Schaefer for the radiation measurements at Glaciar Mocho, and W. J. van den Berg for his help with the analysis of the ERA-reanalysis data. We thank R. Neukom and two anonymous reviewers for their useful comments and suggestions. This study is supported by the Netherlands Organisation for Scientific Research (NWO), research program 816.01.016.

Edited by: A. Rivera



The publication of this article was sponsored by PAGES.

## References

- Adhikari, S. and Huybrechts, P.: Numerical modelling of historical front variations and the 21st-century evolution of Glacier AX010, Nepal Himalaya, *Ann. Glaciol.*, 50, 27–34, 2009.
- Agostini, A.: Nahuel-Huapí – Bellezas Naturales de los Andes en la Patagonia Septentrional, Estudios Fotográficos, Buenos Aires, Argentina, 1949.
- Andreassen, L. M., Elvehøy, H., Kjølmoen, B., Engeset, R. V., and Haakensen, N.: Glacier mass-balance and length variation in Norway, *Ann. Glaciol.*, 42, 317–325, 2005.
- Boninsegna, J. A., Argollo, J., Aravena, J. C., Barichivich, J., Christie, D., Ferrero, M. E., Lara, A., Le Quesne, C., Luckman, B. H., Masiokas, M., Morales, M., Oliveira, J. M., Roig, F., Srur, A., and Villalba, R.: Dendroclimatological reconstructions in South America: a review, *Palaeogeography, Palaeoclimatology, Palaeoecology*, 281, 210–228, doi:10.1016/j.palaeo.2009.07.020, 2009.
- Boucher, É., Guiot, J., and Chapron, E.: A millennial multi-proxy reconstruction of summer PDSI for Southern South America, *Clim. Past*, 7, 957–974, doi:10.5194/cp-7-957-2011, 2011.
- Bown, F. and Rivera, A.: Climate changes and recent glacier behaviour in the Chilean Lake District, *Global Planet. Change*, 59, 76–86, 2007.
- Bown, F., Rivera, A., Acuña, C., and Casassa, G.: Recent glacier mass balance calculations at Volcán Mocho-Choshuenco ( $40^\circ\text{S}$ ), Chilean Lake District, vol. 318, IAHS Publ., Wallingford, UK, 143–152, 2007.
- Briffa, K. R., Schweingruber, F. H., Jones, P. D., Osborn, T. J., Shiyatov, S. G., and Vaganov, E. A.: Reduced sensitivity of recent tree-growth to temperature at high northern latitudes, *Nature*, 391, 678–682, 1998.
- Briffa, K. R., Osborn, T. J., Schweingruber, F. H., Harris, I. C., Jones, P. D., Shiyatov, S. G., and Vaganov, E. A.: Low-frequency temperature variations from a northern tree ring density network, *J. Geophys. Res.*, 106, 2929–2941, 2001.
- Brock, B., Rivera, A., Casassa, G., Bown, F., and Acuña, C.: The surface energy balance model of an active ice-covered volcano: Villarrica Volcano, southern Chile, *Ann. Glaciol.*, 45, 104–114, 2007.

- Bromwich, D. H. and Fogt, R. L.: Strong trends in the skill of the ERA-40 and NCEP-NCAR reanalyses in the high and midlatitudes of the Southern Hemisphere, 1958–2001, *J. Climate*, 17, 4603–4619, 2004.
- Brugger, K. A.: The non-synchronous response of Rabots Glaciär and Storglaciären, northern Sweden, to recent climate change: a comparative study, *Ann. Glaciol.*, 46, 275–282, 2007.
- Budd, W. F., Keage, P. L., and Blundy, N. A.: Empirical studies of ice sliding, *J. Glaciol.*, 23, 157–170, 1979.
- Carrasco, J. F., Osorio, R., and Casassa, G.: Secular trend of the equilibrium-line altitude on the western side of the southern Andes, derived from radiosonde and surface observations, *J. Glaciol.*, 54, 538–550, 2008.
- Christensen, J. H., Hewitson, B., Busuioc, A., Chen, A., Gao, X., Held, I., Jones, R., Kolli, R. K., Kwon, W.-T., Laprise, R., Magaña Rueda, V., Mearns, L., Menéndez, C. G., Räisänen, J., Rinke, A., Sarr, A., and Whetton, P.: Regional climate projections, in: *Climate Change 2007: The Physical Science Basis. Contribution of Working Group I to the fourth Assessment Report of the Intergovernmental Panel on Climate Change*, edited by: Solomon, S., Qin, D., Manning, M., Chen, Z., Marquis, M., Averyt, K. B., Tignor, M., and Miller, H. L., Cambridge University Press, Cambridge, UK and New York, NY, USA, 2007.
- Condom, T., Coudrain, A., Sicart, J. E., and Théry, S.: Computation of the space and time evolution of equilibrium-line altitudes on Andean glaciers (10° N–55° S), *Global Planet. Change*, 59, 189–202, 2007.
- Cook, E. R. and Kairiukstis, L. A. (Eds.): *Methods of dendrochronology, applications in the environmental sciences*, Kluwer Academic Publishers, Dordrecht, The Netherlands, 1990.
- Cook, K. H., Yang, X., Carter, C. M., and Belcher, B. N.: A modeling system for studying climate controls on mountains glaciers with application to the Patagonian Icefields, *Climatic Change*, 56, 339–367, 2003.
- Esper, J., Cook, E. R., and Schweingruber, F. H.: Low-frequency signals in long tree-ring chronologies for reconstructing past temperature variability, *Science*, 295, 2250–2253, 2002.
- Farr, T. G., Rosen, P. A., Caro, E., Crippen, R., Duren, R., Hensley, S., Kobrick, M., Paller, M., Rodriguez, E., Roth, L., Seal, D., Shaffer, S., Shimada, J., Umland, J., Werner, M., Oskin, M., Burbank, D., and Alsdorf, D.: The Shuttle Radar Topography mission, *Rev. Geophys.*, 45, 8755–1209, doi:10.1029/2005RG000183, 2007.
- Fonk, F.: *Diario del Fray Francisco Menéndez a la Cordillera*, Colección Biblioteca Nacional, Valparaiso, Chile, 1886.
- Gallopín, G. C.: Estudio Ecológico integrado de la cuenca del Río Manso Superior, (Río Negro, Argentina), Part I, Descripción general de la cuenca, in: *Anales de Parques Nacionales*, vol. XIV, Servicio Nacional de Parques Nacionales, Buenos Aires, Argentina, 161–230, 1978.
- Giesen, R. H. and Oerlemans, J.: Response of the ice cap Hardangerjøkulen in southern Norway to the 20th and 21st century climates, *The Cryosphere*, 4, 191–213, doi:10.5194/tc-4-191-2010, 2010.
- Giesen, R. H. and Oerlemans, J.: Global application of a surface mass balance model using gridded climate data, *The Cryosphere Discuss.*, 6, 1445–1490, doi:10.5194/tcd-6-1445-2012, 2012.
- Greuell, W.: Hintereisferner, Austria: mass-balance reconstruction and numerical modelling of the historical length variations, *J. Glaciol.*, 38, 233–244, 1992.
- Harrison, S., Winchester, V., and Glasser, N.: The timing and nature of recession of outlet glaciers of Hielo Patagónico Norte, Chile, from their Neoglacial IV (Little Ice Age) maximum positions, *Global Planet. Change*, 59, 67–78, doi:10.1016/j.gloplacha.2006.11.020, 2007.
- Hock, R. and Holmgren, B.: A distributed surface energy-balance model for complex topography and its application to Storglaciären, Sweden, *J. Glaciol.*, 51, 25–36, 2005.
- Iqbal, M.: *An Introduction to Solar Radiation*, Academic Press, 1983.
- Jarvis, A., Rubiano, J., Nelson, A., Farrow, A., and Mulligan, M.: Practical use of the SRTM data in the tropics – Comparisons with digital elevation models generated from cartographic data, in: *Working Document 198, Centro Internacional de Agricultura Tropical*, Cali, Colombia, p. 32, 2004.
- Jóhannesson, T., Raymond, C., and Waddington, E.: Time-scale for adjustment of glaciers to changes in mass balance, *J. Glaciol.*, 35, 355–369, 1989.
- Lara, A., Villalba, R., and Urrutia, R.: A 400-year tree-ring record of the Puelo River summer–fall streamflow in the Valdivian Rainforest eco-region, Chile, *Climatic Change*, 86, 331–356, doi:10.1007/s10584-007-9287-7, 2008.
- Laumann, T. and Nesje, A.: The impact of climate change on future frontal variations of Briksdalsbreen, western Norway, *J. Glaciol.*, 55, 789–796, 2009.
- Leclercq, P. W. and Oerlemans, J.: Global and hemispheric temperature reconstruction from glacier length fluctuations, *Clim. Dynam.*, 38, 1065–1079, doi:10.1007/s00382-011-1145-7, 2012.
- Luckman, B. H.: The Little Ice Age in the Canadian Rockies, *Geomorphology*, 32, 357–384, doi:10.1016/S0169-555X(99)00104-X, 2000.
- Masiokas, M. H., Rivera, A., Espizúa, L. E., Villalba, R., Delgado, S., and Aravena, J. C.: Glacier fluctuations in extratropical South America during the past 1000 years, *Palaeogeogr. Palaeoclimatol.*, 281, 242–268, doi:10.1016/j.palaeo.2009.08.006, 2009.
- Masiokas, M. H., Luckman, B. H., Villalba, R., Ripalta, A., and Rabassa, J.: Little Ice Age fluctuations of Glaciar Río Manso in the north Patagonian Andes of Argentina, *Quatern. Res.*, 73, 96–106, doi:10.1016/j.yqres.2009.08.004, 2010.
- National Climate Data Center, NOAA: *Global Historical Climatology Network version 2*, 2011.
- Neukom, R., Luterbacher, J., Villalba, R., Küttel, M., Frank, D., Jones, P. D., Grosjean, M., Esper, J., Lopez, L., and Wanner, H.: Multi-centennial summer and winter precipitation variability in southern South America, *Geophys. Res. Lett.*, 37, L14708, doi:10.1029/2010GL043680, 2010.
- Neukom, R., Luterbacher, J., Villalba, R., Küttel, M., Frank, D., Jones, P. D., Grosjean, M., Wanner, H., Aravena, J. C., Black, D. E., Christie, D. A., D’Arrigo, R., Lara, A., Morales, M., Soliz-Camboa, C., Srur, S., Urrutia, R., and von Gunten, L.: Multiproxy summer and winter surface air temperature field reconstructions for southern South America covering the past centuries, *Clim. Dynam.*, 37, 35–51, doi:10.1007/s00382-010-0793-3, 2011.

- Nussbaumer, S. U., Nesje, A., and Zumbühl, H. J.: Historical glacier fluctuations of Jostedalsbreen and Folgefonna (southern Norway) reassessed by new pictorial and written evidence, *Holocene*, 21, 455–471, doi:10.1177/0959683610385728, 2011.
- Oerlemans, J.: The mass balance of the Greenland ice sheet: sensitivity to climate change as revealed by energy-balance modelling, *Holocene*, 1, 40–48, 1991.
- Oerlemans, J.: A flow-line model for Nigardsbreen: projection of future glacier length based on dynamic calibration with the historic record, *Ann. Glaciol.*, 24, 382–389, 1997a.
- Oerlemans, J.: Climate sensitivity of Franz Josef Glacier, New Zealand, as revealed by numerical modelling, *Arct. Alpine Res.*, 29, 233–239, 1997b.
- Oerlemans, J.: *Glaciers and Climate Change*, AA Balkema Publishers, 2001.
- Oerlemans, J.: Extracting a climate signal from 169 glacier records, *Science*, 308, 675–677, 2005.
- Oerlemans, J.: *The microclimate of valley glaciers*, Igitur, Utrecht Publishing & Archiving Services, Universiteitsbibliotheek Utrecht, 2010.
- Oerlemans, J. and Knap, W. H.: A 1 year record of global radiation and albedo in the ablation zone of Morteratschgletscher, Switzerland, *J. Glaciol.*, 44, 231–238, 1998.
- Oerlemans, J. and Reichert, B. K.: Relating glacier mass balance to meteorological data using a Seasonal Sensitivity Characteristic (SSC), *J. Glaciol.*, 46, 1–6, 2000.
- Oerlemans, J., Anderson, B., Hubbard, A., Huybrechts, P., Jóhannesson, T., Knap, W. H., Schmeits, M., Stroeven, A. P., van de Wal, R. S. W., Wallinga, J., and Zuo, Z.: Modelling the response of glaciers to climate warming, *Clim. Dynam.*, 14, 267–274, 1998.
- Peterson, T. C. and Vose, R. S.: An overview of the Global Historical Climatology Network temperature database, *B. Am. Meteorol. Soc.*, 78, 2837–2849, 1997.
- Rivera, A., Bown, F., Casassa, G., Acuña, C., and Clavero, J.: Glacier shrinkage and negative mass balance in the Chilean Lake District (40° S), *Hydrolog. Sci. J.*, 50, 963–974, doi:10.1623/hysj.2005.50.6.963, 2005.
- Rosenblüth, B., Fuenzaliba, H. A., and Aceituno, P.: Recent temperature variations in southern South America, *Int. J. Climatol.*, 17, 67–85, 1997.
- Ruiz, L., Masiokas, M. H., and Villalba, R.: Fluctuations of Glaciar Esperanza Norte in the north Patagonian Andes of Argentina during the past 400 yr, *Clim. Past*, 8, 1079–1090, doi:10.5194/cp-8-1079-2012, 2012.
- Rye, C. J., Arnold, N. S., Willis, I. C., and Kohler, J.: Modelling the surface mass balance of high Arctic glacier using the ERA-40 reanalysis, *J. Geophys. Res.*, 115, F02014, doi:10.1029/2009JF001364, 2010.
- Simmons, A., Uppala, S., Dee, D., and Kobayashi, S.: ERA-Interim: new ECMWF reanalysis products from 1989 onwards, *ECMWF Newsletter*, 110, 25–35, 2006.
- Stroeven, A., van de Wal, R., and Oerlemans, J.: Historic front variations of the Rhone Glacier: simulation with an ice flow model, in: *Glacier fluctuations and climate change, edited by: Oerlemans, J., Glaciology and quaternary geology*, Kluwer Academic Publishers, Dordrecht, The Netherlands, 1989.
- Vera, C., Silvestri, G., Liebmann, B., and González, P.: Climate change scenarios for seasonal precipitation in South America from IPCC-AR4 models, *Geophys. Res. Lett.*, 33, L13707, doi:10.1029/2006GL025759, 2006.
- Villalba, R., Leiva, J. C., Rubulls, S., Suarez, J., and Lenzano, L.: Climate, tree-ring and glacial fluctuations in the Rio Frías Valley, Rio Negro, Argentina, *Arct. Alpine Res.*, 22, 215–232, 1990.
- Villalba, R., Boninsegna, J. A., Veblen, T. T., Schmelter, A., and Rubulis, S.: Recent trends in tree-ring records from high elevation sites in the Andes of northern Patagonia, *Climatic Change*, 36, 425–454, 1997.
- Villalba, R., Cook, E. R., Jacoby, G. C., D'Arrigo, R. D., Veblen, T. T., and Jones, P. D.: Tree-ring based reconstructions of northern Patagonia precipitation since AD 1600, *Holocene*, 8, 659–674, doi:10.1191/095968398669095576, 1998.
- Villalba, R., Lara, A., Boninsegna, J. A., Masiokas, M. H., Delgado, S., Aravena, J. C., Roig, F. A., Schmelter, A., Wolodarsky, A., and Ripalta, A.: Large-scale temperature changes across the southern Andes: 20th-century variations in the context of the past 400 years, *Climatic Change*, 59, 177–232, 2003.
- WGMS: *Fluctuations of Glaciers*, vol. IX, ICSU (FAGS)/IUGG(IACS)/UNEP/UNESCO/WMO, updated, and earlier volumes, World Glacier Monitoring Service, Zurich, Switzerland, 2008.
- Zumbühl, H. J. and Holzhauser, H.: *Alpengletscher in der Kleinen Eiszeit*, vol. 3 of *Die Alpen*, Schweizerischen Alpen Club, Bern, Switzerland, 1988.